



Artificial micro-swimmers in simulated natural environments

 Cite this: *Lab Chip*, 2016, 16, 1101

 J. Katuri,^{ac} K. D. Seo,^b D. S. Kim^b and S. Sánchez^{*acd}

Microswimmers, such as bacteria, are known to show different behaviours depending on their local environment. They identify spatial chemical gradients to find nutrient rich areas (chemotaxis) and interact with shear flows to accumulate in high shear regions. Recently, artificial microswimmers have been developed which mimic their natural counterparts in many ways. One of the exciting topics in this field is to study these artificial motors in several natural settings like the ones bacteria interact with. In this Focus article, we summarize recent observations of artificial swimmers in chemical gradients, shear flows and other interesting natural environments simulated in the lab using microfluidics and nanotechnology.

DOI: 10.1039/c6lc90022d

www.rsc.org/loc

One of the important advances in colloidal physics over the last decade has been the development of self-propelled colloids.¹ These are micron sized particles that transduce free energy from their surroundings and engage in directed motion, much like bacteria. While bacteria use flagellar motion as a strategy to perform directed motion, phoretic mechanisms have been preferred for the colloids developed in the lab. Phoresis (from Greek ‘phorein’, which means ‘to carry’) is the general term used to refer to the migration of colloidal particles over different thermodynamic gradients. Self-propelled particles, like Janus particles, use differential chemical reactions on their surface to generate chemical gradients in which they propel. A number of applications have been conceived for these particles, ranging from targeted drug delivery to environmental remediation, and some of them have already been demonstrated.²

While the properties of an individual colloidal swimmer are fairly well understood, the effort to study their behaviour in dynamic environments such as externally imposed chemical gradients and shear flows has only recently begun. These studies are of great interest as natural micro-swimmers such as *Escherichia coli* bacteria respond to chemical gradients, evident in their chemotactic motion to find nutrient rich areas, and sperm cells exhibit upstream mobility (positive rheotaxis) under shear flow which is thought to be one of the guiding mechanisms in their motion towards the ovum.

Synthetic micro-swimmers are known to mimic the behaviour of their natural counterparts in many ways, such as exhibiting persistent random walk and engaging in collective behaviour, and could possibly present similarities when exposed to gradients and flow fields as well. Another area of interest is to study the interactions of these phoretic swimmers with static environments such as surfaces, walls,³ patterned obstacles^{4,5} and ratchets,⁶ as potential applications of these particles involve their motion in complex environments.

Recent progress in microfluidics and nanotechnology has enabled scientists to simulate naturally occurring environments with great control in the lab. In this article, we summarize recent observations ranging from migration of synthetic swimmers in chemical gradients, to their response to shear flow and gravity.

Studying colloidal particles and enzymes in chemical gradients

A number of strategies have been used to create chemical gradients in the lab.⁷ One of the general approaches is to use convection based gradient generators such as the T junction (Fig. 1A) which rely only on the micro-channel geometries to create steady gradients. In experiments where it is preferred not to expose the samples to non-native shear flows, it is common to use diffusion based chemical generators where porous materials such as hydrogels separate the observation channels from the channels carrying the concentrated solutions (Fig. 1A).⁸ While a linear gradient is created in the observation channels, the flows are restricted only to the side channels.

The mechanism by which colloidal particles migrate along concentration gradients is called diffusiophoresis.

^a Max Planck Institute for Intelligent Systems, Heisenbergstrasse 3, 70569, Stuttgart, Germany. E-mail: sanchez@is.mpg.de

^b Department of Mechanical Engineering, POSTECH (Pohang University of Science and Technology), Pohang, Gyeongbuk, 790-784 Korea

^c Institute for Bioengineering of Catalonia (IBEC), Baldri I Reixac 10-12, 08028 Barcelona, Spain. E-mail: ssanchez@ibecbarcelona.eu

^d Catalan Institute for Research and Advanced Studies (ICREA), Psg. Lluís Companys, 23, 08010 Barcelona, Spain

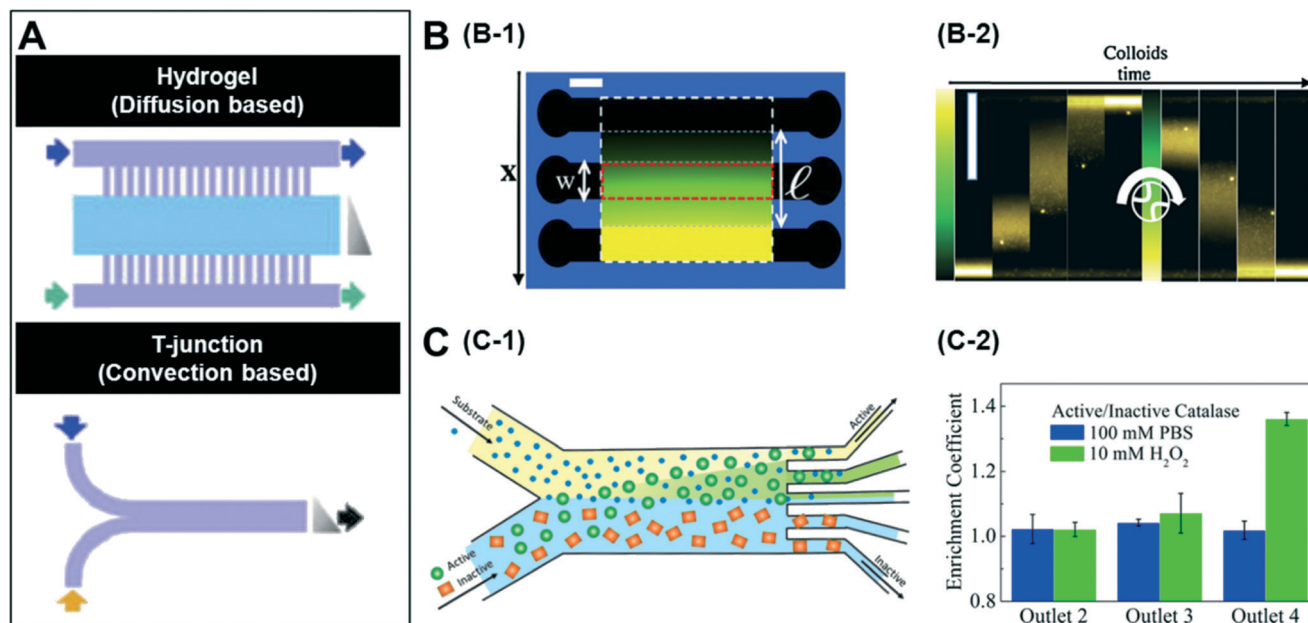


Fig. 1 A. Microfluidic setups to create chemical gradients. The lower panel represents convection based gradient generators and the upper panel is diffusion based. The grey triangle represents the shape of the gradient and arrows indicate flow direction. B. Diffusiophoretic migration of colloids in a salt gradient. B-1 is the schematic of a three channel microfluidic chip moulded in agarose gel. A linear chemical gradient is created in the central channel due to diffusion from the side channels where the salt solution is flowed. B-2 contains time lapse images showing the migration of colloids in a LiCl gradient. C. Chemotactic separation of enzymes. C-1 is the schematic of a two-inlet/five-outlet chip used to separate enzymes based on their activity. C-2 is the measured enrichment coefficients of urease and catalase within different outlets of the device. Reprinted from ref. 7 (A), ref. 9 (B) and ref. 10 (C) with permission.

Diffusiophoretic transport of colloidal particles was demonstrated by Palacci *et al.* who implemented a three channel microfluidic set-up (Fig. 1B-1) to impose both stationary and temporally switchable solute gradients.⁹ The side channels are connected to a double syringe pump with solutions of salt concentrations and a linear concentration gradient is established in the observation channel by the diffusion of the solute through porous membranes located in the side walls. When the authors started with a configuration where all the particles were on one side of the channel and the LiCl salt gradient was turned on, they observed the migration of colloids towards the higher solute concentration (Fig. 1B-2). The drift velocity (V_D) of the colloidal particles is related to their mobility (μ) and the concentration gradient (∇c) as, $V_D = \mu \nabla c$ and as expected, the observed drift was close to linear. Similar results were observed when they used λ -DNA instead of colloidal particles.

Recently there has been significant interest in studying enzymes as active materials. Based on their chemotactic behaviour, Dey *et al.* demonstrated a method to separate enzymes using an imposed substrate concentration gradient.¹⁰ In this case they used a two-inlet/five-outlet convection based channel (Fig. 1C-1) to separate active and inactive enzymes in particular substrates. Fig. 1C-2 shows the results from an experiment where the authors flowed catalase and urease in a 1:1 mixture through one of the substrates. When 10 mM H₂O₂, which is a substrate for catalase but not urease, was flowed through the other channel, a significant enrichment of

catalase was found in outlet 4 due to deviation of catalase towards the peroxide flow. Similar separation of urease from β -galactosidase was achieved by using urea as a substrate.

Chemotactic behaviour of artificial micro-swimmers

While the concentration gradient in the above system was externally imposed, lately, colloids which create their own concentration gradient have been developed. Generally, these are silica/polystyrene micro particles which are half coated with a layer of Pt. When these colloids are dispersed in a H₂O₂ solution, the Pt side of the particle catalyses the degradation of peroxide and the silica side remains inert. This asymmetric distribution of reaction products on the particle surface establishes a chemical gradient along the particle body, leading to self-propulsion. Baraban *et al.* studied the chemotactic behaviour of spherical and tubular catalytic particles towards H₂O₂.¹¹ They developed a three-inlet parallel flow device (Fig. 2A) where the self-propelled colloids were flowed through the central channel and aqueous solutions in the other two channels. When H₂O₂ was flowed through one of the side channels and water in the other, the motors deviated from the centre towards the channel with the peroxide flow (Fig. 2A). They also observed that the deviation of Janus particles was higher than what was observed for tubular motors, indicating that shape and geometry could play a critical role in the chemotactic behaviour of micro-swimmers.

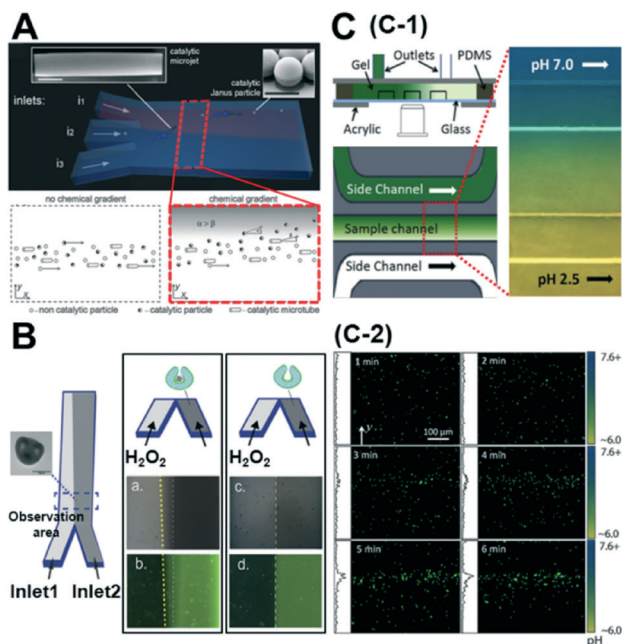


Fig. 2 A. Chemotactic behaviour of chemical micro-swimmers. The top panel is the schematic of a three-inlet/one-outlet microfluidic chip to create a peroxide gradient. Insets are the SEM images of a microjet and a Janus particle. Scale bars represent 5 μm . The bottom panel represents the deviation of the motors towards the channel with peroxide. B. Chemotactic behaviour of 'stomatocyte' nanomotors. Left: Schematic of the two-inlet/one-outlet chip to create a peroxide gradient and the SEM image of the stomatocyte motors. Right: While the stomatocytes loaded with PtNP show a deviation towards the peroxide channel, no deviation is observed in particles without PtNP. C. pH taxis of bio-hybrid micromotors. C-1 is the diffusion based microfluidic channel to create a pH gradient. C-2 shows the bi-directional drift of the bacteria-polystyrene bio-hybrid system away from the more acidic and basic regions. Reprinted from ref. 11 (A), ref. 12 (B) and ref. 13 (C) with permission.

Peng *et al.* observed similar results for their 'stomatocyte' nanomotors which were significantly smaller (~ 300 nm) than the micron-range motors used above.¹² They could demonstrate that their motors, functionalized with Pt nanoparticles (PtNP) and loaded with an anti-cancer drug, showed preferential motion towards higher peroxide concentrations. They used a single path chemotaxis channel where the particles and peroxide were added to the opposite chambers. The observations were made along the connecting path of the channel where a peroxide gradient is established. They recorded that the 'stomatocyte' nanomotors gradually drift towards the chamber with the peroxide concentration and the velocity of this motion was dependent on the concentration of peroxide used. Further, they used a two-inlet channel (Fig. 2B) to demonstrate similar deviations towards higher peroxide concentrations as Baraban *et al.* Such chemotactic behaviour of nanomotors can be exploited to build active drug-delivery vehicles whose motion is guided towards diseased cells based on chemical gradients.

One of the disadvantages of the above described colloidal motors is the need to use H_2O_2 as a fuel. From a practical

point of view, this renders these systems unsuitable for biological applications. While there have been several strategies to overcome this drawback, one of the most promising ones has been to develop bio-hybrid motors. These are colloids that are coupled to a biological swimmer, like a bacteria or a sperm, to derive propulsion. Zhuang *et al.* recently demonstrated pH-taxis in one such system.¹³ They used a bio-hybrid system composed of polystyrene beads and bacteria. In order to create a gradient they used a diffusion based microfluidic set-up (Fig. 2C-1) similar to the one used by Palacci *et al.*⁹ Using a gradient between pH = 6.0 and pH = 7.6, they could show that the bacteria moved away from both strongly acidic and strongly basic areas. Within 5 min after imposing the gradient, the motors formed a concentration band at slightly above pH = 7.0 (Fig. 2C-2). This reversing rate bias at high and low pH was attributed to the pH dependence of the flagellar tumbling rate. At unfavourable pH, bacteria tend to increase their tumbling rate therefore reducing their swimming consistency as compared to the favourable pH regions.

Simulating natural environments to study self-propelled particles

So far, we have focussed our discussion on creating chemical gradients and studying active particles in these gradients. There has also been significant effort to simulate natural settings and demonstrate some of the effects that natural micro-swimmers exhibit. For instance, paramecium protozoa demonstrate negative gravitaxis, *i.e.*, swimming against gravity.¹⁴ With advances in lithography techniques, it is possible to create micron-sized, shape-asymmetric swimmers that help us understand such effects. ten Hagen *et al.* demonstrated that simple shape asymmetry is sufficient to create a negative gravitactic swimmer.¹⁵ They synthesized L shaped particles and coated the front side of the short arm with a gold layer (Fig. 3A-1). Under laser illumination in a binary mixture of water and 2, 6 lutidine at critical temperature, these swimmers propel due to the demixing of the solvent near the gold layer which causes a diffusiophoretic propulsion force normal to the plane of the gold layer. Without propulsion, they noticed that these swimmers sediment under gravity with an orientation angle of -34° (Fig. 3A-2). However, upon illumination, these asymmetric particles swim upwards, against gravity. The shape of this upward trajectory could further be controlled by the illumination strength of the laser (Fig. 3A-3). Since these particles have homogeneous mass distribution, the gravitactic behaviour is purely shape induced.

Another natural system ubiquitous in nature is shear flow. Studying bacteria, Rusconi *et al.* demonstrated that shear flow produces strong spatial heterogeneity by depleting bacteria from the low shear regions and trapping them in high shear regions.¹⁶ They used a serpentine micro-channel to create a shear flow in their experiments (Fig. 3B-1). Initially the bacteria cells are uniformly distributed, but when the flow is induced, they noticed that the concentration depletes in the central part of the channel and accumulates at the flanks in

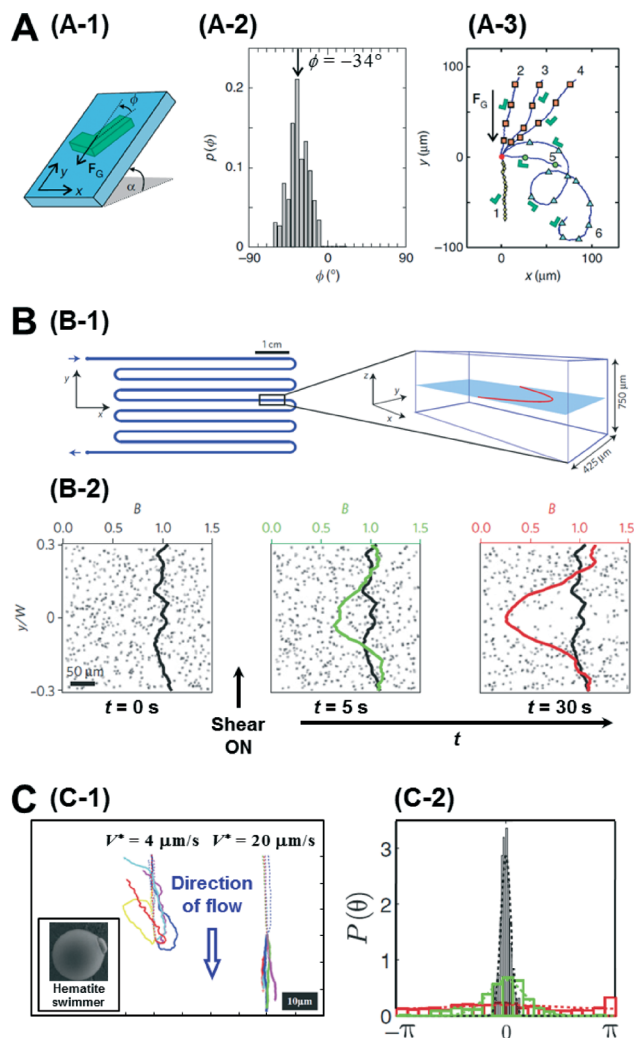


Fig. 3 A. Gravitactic behaviour of shape-asymmetric micromotors. A-1 is the schematic of the L shaped swimmer in a gravitational field. A-2 shows the probability distribution of the sedimentation angle, which has a clear peak at -34° . A-3 shows the swimming trajectories of the asymmetric particles under different intensities of illumination. B. Trapping of bacterial trajectories in high shear regions. B-1 shows the schematic of the serpentine channel used to create the shear flow whose profile is also plotted on the right. B-2 shows the temporal evolution of the concentration profile of bacteria before and after the shear is turned on. C. Artificial rheotaxis. C-1 shows the trajectories of the self-propelled particles in two different flow rates. Inset is the SEM image of the 'hematite' swimmer. C-2 shows the probability distribution of the orientation angle in increasing flow rates (red-black). Reprinted from ref. 15 (A), ref. 16 (B) and ref. 17 (C) with permission.

the high shear region (Fig. 3B-2). This effect could be explained by analysing the individual trajectories of bacteria in regions of high and low shear. In the high shear regions they noticed frequent loops in the bacterial trajectories due to hydrodynamic torque which resulted in a net accumulation in the region. Further, when the authors exposed the bacteria to both shear flow and an oxygen gradient simultaneously, they could show that the trapping effect of the shear flow severely curtails their chemotactic response, suggesting

that accurate chemotaxis experiments need to decouple flow from the system.

Artificial micromotors show another interesting effect when exposed to shear flows. Rheotaxis is the migration of particles in response to shear flow. Bacteria and sperms exhibit positive rheotaxis (upstream migration) caused by the interplay between the velocity gradient and the shape of their flagella. Palacci *et al.* could demonstrate positive rheotaxis in their artificially synthesised 'hematite' swimmers which are not propelled by flagellar motion but rather by self-diffusiophoresis.¹⁷ These swimmers are composed of a hematite cube on a polymer sphere (Fig. 3C-1), and when exposed to blue light in H_2O_2 solution, owing to the decomposition of peroxide by the hematite cube, they set up an osmotic pumping flow along the surface across which the particles surf. The hematite cube is attracted to the bottom surface inducing a polarity in the particle. When exposed to a flow, without activity, these particles roll down along the flow direction as expected. However when self-propulsion is switched on, they orient against the direction of flow and swim upwards (Fig. 3C-1). This alignment is also dependent on the flow rate with higher flows resulting in better alignment (Fig. 3C-2). This effect was explained to be due to a physical mechanism involving the interplay between the polarity of the particles and the viscous torque of the flow. Engineering particles that have specific responses to their environment depending on their intrinsic properties, such as shape and mechanism of motion, represents a further advance in the design of intelligent micro-systems.

Conclusions

In this article we have looked at different ways to create chemical gradients using microfluidics and summarized the results of migration of both bare colloids and self-propelled colloids in these gradients. We have further reviewed the effect of shear flow and gravity on asymmetric self-propelled colloids and discussed the relevance of particle geometry in their response to these external fields.

Acknowledgements

This work was supported by the European Research Council (ERC) starting Grant "Lab-in-a-tube and Nanorobotics biosensors; LT-NRBS" [no. 311529] and National Research Foundation of Korea (NRF) grant (no. 2014R1A2A1A01006527, 2011-0030075) funded by the Korean government (MSIP). S. S. thanks the Commission for Universities and Research of the Department of Innovation, Universities, and Enterprise of the Generalitat de Catalunya (2014 SGR 1442).

Notes and references

- 1 J. R. Howse, R. A. L. Jones, A. J. Ryan, T. Gough, R. Vafabakhsh and R. Golestanian, *Phys. Rev. Lett.*, 2007, **99**, 048102.

- 2 S. Sánchez, L. Soler and J. Katuri, *Angew. Chem., Int. Ed.*, 2015, **54**, 1414–1444.
- 3 S. Das, A. Garg, A. I. Campbell, J. Howse, A. Sen, D. Velegol, R. Golestanian and S. J. Ebbens, *Nat. Commun.*, 2015, **6**, 8999.
- 4 G. Volpe, I. Buttinoni, D. Vogt, H.-J. Kümmerer and C. Bechinger, *Soft Matter*, 2011, **7**, 8810–8815.
- 5 J. Simmchen, J. Katuri, W. E. Uspal, M. Popescu, M. Tasinkevych and S. Sanchez, *Nat. Commun.*, DOI: 10.1038/ncomms10598.
- 6 C. Maggi, J. Simmchen, F. Saglimbeni, J. Katuri, M. Dipalo, F. De Angelis, S. Sanchez and R. Di Leonardo, *Small*, 2015, **12**, 446–451.
- 7 A. G. G. Toh, Z. P. Wang, C. Yang and N.-T. Nguyen, *Microfluid. Nanofluid.*, 2013, **16**, 1–18.
- 8 J. Diao, L. Young, S. Kim, E. A. Fogarty, S. M. Heilman, P. Zhou, M. L. Shuler, M. Wu and M. P. DeLisa, *Lab Chip*, 2006, **6**, 381–388.
- 9 J. Palacci, B. Abécassis, C. Cottin-Bizonne, C. Ybert and L. Bocquet, *Phys. Rev. Lett.*, 2010, **104**, 138302.
- 10 K. K. Dey, S. Das, M. F. Poyton, S. Sengupta, P. J. Butler, P. S. Cremer and A. Sen, *ACS Nano*, 2014, **8**, 11941–11949.
- 11 L. Baraban, S. M. Harazim, S. Sanchez and O. G. Schmidt, *Angew. Chem., Int. Ed.*, 2013, **52**, 5552–5556.
- 12 F. Peng, Y. Tu, J. C. M. van Hest and D. A. Wilson, *Angew. Chem.*, 2015, **127**, 11828–11831.
- 13 J. Zhuang, R. Wright Carlsen and M. Sitti, *Sci. Rep.*, 2015, **5**, 11403.
- 14 A. M. Roberts, *J. Exp. Biol.*, 2010, **213**, 4158–4162.
- 15 B. ten Hagen, F. Kümmel, R. Wittkowski, D. Takagi, H. Löwen and C. Bechinger, *Nat. Commun.*, 2014, **5**, 4829.
- 16 R. Rusconi, J. S. Guasto and R. Stocker, *Nat. Phys.*, 2014, **10**, 212–217.
- 17 J. Palacci, S. Sacanna, A. Abramian, J. Barral, K. Hanson, A. Y. Grosberg, D. J. Pine and P. M. Chaikin, *Sci. Adv.*, 2015, **1**, e1400214.